Journal of Molecular Liquids 392 (2023) 123431

Contents lists available at ScienceDirect

Journal of Molecular Liquids

journal homepage: www.elsevier.com/locate/molliq

Physicochemical characterization of hydrophobic type III and type V deep eutectic solvents based on carboxylic acids

Alaine Duque [a], Antton Sanjuan [b], M. Mounir Bou-Ali [b], Rosa M. Alonso [c,*], Miguel A. Campanero [a]

[a] A3Z Advanced Analytical Consulting Services, 48160 Derio, Vizcaya, Spain
[b] Fluid Mechanics Group, Mechanical and Manufacturing Department, Faculty of Engineering, Mondragon University, 20500 Arrasate-Mondragon, Spain
[c] FARMARTEM Group, Department of Analytical Chemistry, Faculty of Science and Technology, University of the Basque Country (UPV/EHU), 48940 Leioa, Vizcaya, Spain

ARTICLE INFO

Keywords:
Deep eutectic solvent
Physicochemical characterization
UV filters
Dispersive liquid–liquid microextraction
Water samples

ABSTRACT

In the present work, novel type III and type V deep eutectic solvents (DESs) were prepared by mixing choline chloride (ChCl), tetrabutylammonium chloride (TBAC) or thymol as HBA, and different alkyl chain length carboxylic acids as HBD (acetic, oxalic, palmitic, stearic, oleic and linoleic acid) at various molar ratios. The hydrophobic DESs were characterized by infrared spectroscopy (FT-IR) and proton nuclear magnetic resonance (^{1}H NMR), concluding the formation of intermolecular interactions, as hydrogen bonds between the precursors. Thermogravimetric analysis (TGA) was used to obtain the thermal decomposition profiles of the prepared DESs, proving interactions between the precursors and decomposition temperatures with values, which are found in the ranges of the precursor constituents and higher than 170 °C. Other physicochemical properties, such as density, thermal expansion coefficient, dynamic viscosity, refractive index, surface tension, and thermal and ionic conductivities have been determined. Furthermore, the ability of these DESs as UV filter extractants from aqueous samples using a dispersive liquid–liquid microextraction (DLLME) previous to liquid chromatographic analysis was demonstrated. Therefore, these type III and type V DESs could be applied to the extraction of pollutants from environmental water samples.

1. Introduction

Deep eutectic solvents (DESs) have recently emerged as novel alternative to conventional solvents [1,2] in multiple areas, such as extraction procedures [3], pharmaceutical formulation [4] or biomass processing [5]. DESs are typically formed by mixing a hydrogen bond acceptor (HBA) and a hydrogen bond donor (HBD), forming a liquid with a melting point lower than that of the individual components and strong hydrogen bond interactions [6]. There are several methods which allow the successful preparation of DESs, as stirring and heating [7], vacuum evaporation [8], grinding [9], freeze drying [10], twin screw extrusion [11], microwave irradiation [12] and ultrasound assisted methods [13]. Among the methods, stirring and heating, and grinding are the most widely used for preparation of DESs due to their simplicity of the process [14]. The opportunity of designing the most suitable DESs with the election of their individual components, make them an encouraging option for being applied in several fields. Furthermore, their individual components are low cost and present low toxicity [15].

DESs can be classified based on their composition (type I-V) or according to the nature of the individual constituents (natural deep eutectic solvents or therapeutic deep eutectic solvents). Type I and type II DESs are prepared with the combination of a quaternary ammonium salt and a metal chloride, in anhydrous (type I) or hydrated form (type II) [16]. Type III DESs, which are the most studied type of DESs, are usually prepared using quaternary ammonium salt as HBA and organic molecules (carboxylic acids or alcohols) as HBD [17]. Type IV comprise of a combination between type I or II and type III DESs. Herein, the eutectic mixture is formed with a metal chloride/metal chloride hydrate as HBA and an organic molecule as HBD [6]. In addition, a new class of DESs has been recently incorporated in the classification (type V) combining non-ionic organic molecules as HBA and HBD [18,19]. This is a promising variety since it is consisted of environmentally friendly components and there is a wide choice of non-ionic substances that may be employed for the formulation of DESs with different degrees of

* Corresponding author.
E-mail address: rosamaria.alonso@ehu.eus (R.M. Alonso).

https://doi.org/10.1016/j.molliq.2023.123431
Received 28 June 2023; Received in revised form 6 October 2023; Accepted 24 October 2023
Available online 27 October 2023

hydrophobicity.

DESs are formed through hydrogen bonding between acceptor and donor compounds, as well as other intermolecular interactions such as Van der Waals and electrostatic forces. These interactions among the precursors lead to charge delocalization, giving rise to distinct physicochemical properties of DESs that differ from their constituent compounds. Notably, DESs exhibit exceptional characteristics, including low vapour pressure, high thermal stability, low flammability, and a strong solubilization capacity [17]. For the physicochemical characterization of DESs, their hydrogen bonding ability via FT-IR and ^{1}H NMR, degradation temperature by thermogravimetric analysis (TGA), density (ρ), thermal expansion coefficient (α), dynamic viscosity (μ), refractive index (n), surface tension (γ), and thermal (λ) and ionic (k) conductivity are commonly evaluated [20]. Besides the influence of the large variety of components and the effect of their alkyl chain length or ion type, DESs properties can be affected by their molar ratio and purity, temperature, water content and preparation method [21]. The hydrogen bonding is the key intermolecular force between DESs constituents, which is behind the melting point depression occurred during DESs formation [22]. Studies revealed that stronger hydrogen bond interactions correspond to lower melting points [7,23–28].

In recent years, different alkyl chain length carboxylic acids have been employed as HBD in combination with diverse HBAs, since they strongly influence the characteristics of formulated DESs. In this sense, authors demonstrated that some physicochemical properties of DESs as density, degradation temperature, melting point or hydrogen bond strength increased or decreased together with the alkyl chain length, depending on the structure and properties of the HBA and the molar ratio of the components [9,26,29–32].

In this work, novel type III and type V DESs were prepared and physicochemical characterization of the hydrophobic DESs was carried out in order to understand the structure and behaviour of these solvents and to evaluate the effects of the different precursor materials. Precursor components of this study were selected based on their environmental friendliness, low cost and easy acquisition. Type III DESs were comprised of choline chloride (ChCl) or tetrabutylammonium chloride (TBAC) as HBA, otherwise type V DESs were composed of the monoterpene thymol as HBA. Different alkyl chain length carboxylic acids were selected as HBD (i.e., acetic, oxalic, palmitic, stearic, oleic and linoleic acid) to assess their DES formation capacity. Structure of chosen HBAs and HBDs is presented in Fig. 1. Furthermore, dispersive liquid–liquid microextraction (DLLME) coupled to high performance liquid chromatography-variable wavelength detector (HPLC-VWD) methodology, previously developed and validated, was used to demonstrate the ability of these DESs as UV filter extractants from aqueous samples. Future implementation in the analysis of environmental water samples will be carried out to assess the UV filters contaminant effect.

2. Experimental

2.1. Reagents

All reagents and solvents used in this study are of analytical-quality grade. The UV filters benzophenone-3 100 % (BZ3), 4-methylbenzylidene camphor 99.7 % (MBC) and octocrylene > 97 % (OC) from Sigma-Aldrich (Steinheim, Germany) were used as standards.

For the preparation of the different DESs, choline chloride (ChCl) > 98 %, tetrabutylammonium chloride (TBAC) > 97 % and thymol > 99 % purchased to Sigma-Aldrich (Steinheim, Germany) were employed as HBA. Acetic acid glacial (aceA), palmitic acid > 95 % (palA), stearic acid (steA, 95 %, reagent grade), oleic acid (oleA, 90 %, technical grade) and linoleic acid > 95 % (linA) from Sigma-Aldrich (Steinheim, Germany) and oxalic acid (oxaA, anhydrous) from Fisher Scientific (Dreieich, Germany) were used as HBD.

Deuterated chloroform ($CDCl_3$) for ^{1}H NMR experiments was purchased to Sigma-Aldrich (Darmstadt, Germany) and ultrapure water

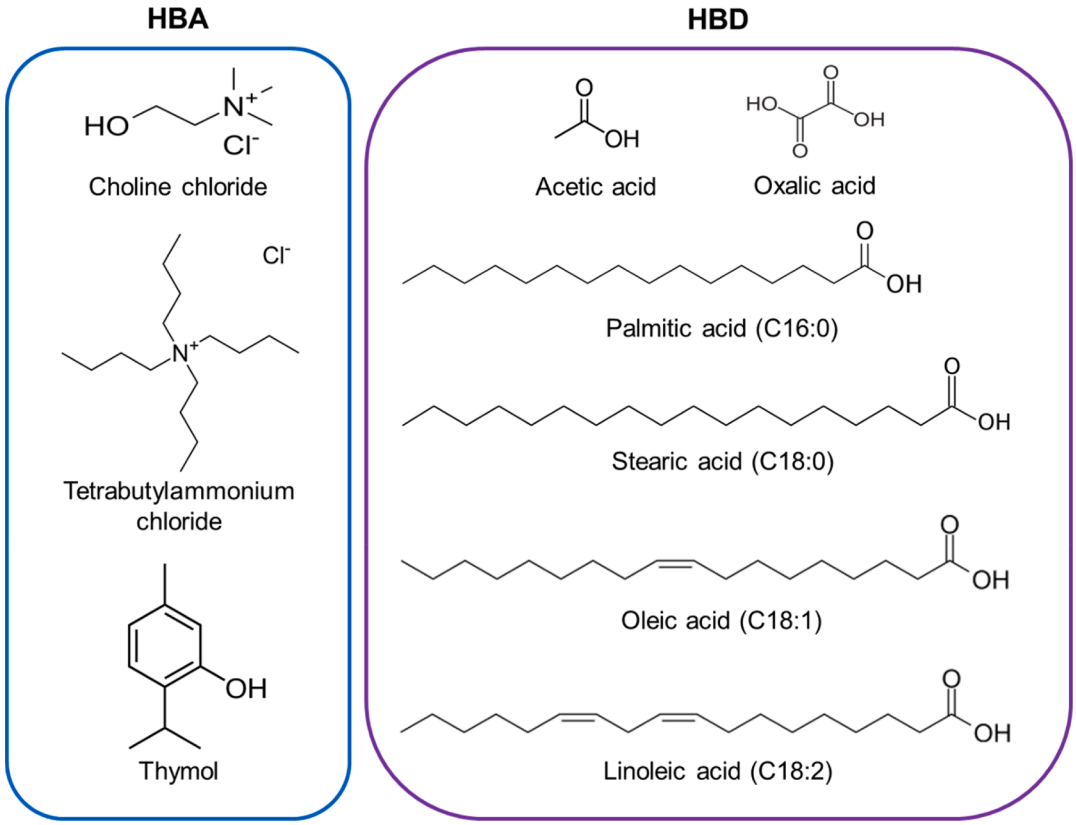

Fig. 1. Different hydrogen bond acceptors (HBA) and hydrogen bond donors (HBD) employed in this work.

used in the experiments was obtained from Milli-Q water purification system (Merck Millipore, Darmstadt, Germany).

The chromatographic mobile phase was prepared using acetic acid (glacial), HPLC-grade acetonitrile and 2-propanol obtained from VWR Chemicals (Fontenay-sous-Bois, France).

2.2. Apparatus

For the DES preparation procedure, a precision analytical balance GRAM FV-220 from Gram (Kolding, Denmark), a WNB 22 water bath from Memmert (Schwabach, Germany) and a Reax top vortex mixer from Heidolph Instruments (Schwabach, Germany) were employed.

A multitube vortexer from Fisher Scientific (Dreieich, Germany) and a Multifuge 3SR centrifuge from Heraeus (Hanau, Germany) were used to perform the DES-based DLLME process.

An Agilent 1100 Series HPLC system equipped with a G1313A autosampler, a G1311A quaternary pump and a G1314A variable wavelength detector (VWD) was employed for the quantitative

Table 1
Organoleptic stability, preparation temperature and water compatibility of the different DESs combinations prepared in this work.

HBA	HBD	Molar ratio	Preparation temperature (°C)	Organoleptic stability	Water compatibility
ChCl	Acetic acid	1:1	95	Precipitate	–
		1:5		Precipitate	–
		5:1		Precipitate	–
	Oxalic acid	1:1	95	Yellow homogenous liquid	Hydrophilic
		1:5		Precipitate	–
		5:1		Precipitate	–
		1:10		Solid	–
	Palmitic acid	1:1	95	Precipitate	–
		1:5		Precipitate	–
		5:1		Solid	–
	Stearic acid	1:1	95	Precipitate	–
		1:5		Solid	–
		5:1		Solid	–
	Oleic acid	1:1	95	Precipitate	–
		1:5		Transparent homogenous liquid	Hydrophilic
		5:1		Solid	–
		1:10		Precipitate (hours)	–
	Linoleic acid	1:1	95	Precipitate	–
		1:5		Precipitate (day 22)	–
		5:1		Precipitate	–
		1:4		Precipitate (minutes)	–
TBAC	Acetic acid	1:1	90	Solid (day 2)	–
		1:5		Transparent homogenous liquid	Hydrophilic
		5:1		Precipitate (minutes)	–
		1:10		Precipitate (hours)	–
	Oxalic acid	1:1	90	Precipitate	–
		1:5		Precipitate	–
		5:1		Precipitate	–
	Palmitic acid	1:1	90	Transparent homogenous liquid	Precipitation
		1:5		Solid	–
		5:1		Transparent homogenous liquid	Precipitation
	Stearic acid	1:1	90	Solid	–
		1:5		Solid	–
		5:1		Solid	–
	Oleic acid	1:1	90	Transparent homogenous liquid	Hydrophobic
		1:5		Transparent homogenous liquid	Hydrophobic
		5:1		Precipitate (hours)	–
		2:1		Transparent homogenous liquid	Precipitation
	Linoleic acid	1:1	90	Yellow homogenous liquid	Hydrophobic
		1:5		Yellow homogenous liquid	Hydrophobic
		5:1		Precipitate (hours)	–
		2:1		Yellow homogenous liquid	Hydrophobic
Thymol	Acetic acid	1:1	60	Transparent homogenous liquid	Precipitation
		1:5		Precipitate	–
		5:1		Transparent homogenous liquid	Precipitation
		1:10		Transparent homogenous liquid	Hydrophilic
	Oxalic acid	1:1	60	Precipitate	–
		1:5		Precipitate	–
		5:1		Precipitate	–
	Palmitic acid	1:1	60	Solid	–
		1:5		Solid	–
		5:1		Solid	–
	Stearic acid	1:1	60	Precipitate	–
		1:5		Precipitate	–
		5:1		Precipitate	–
	Oleic acid	1:1	60	Transparent homogenous liquid	Hydrophobic
		1:5		Transparent homogenous liquid	Hydrophobic
		5:1		Precipitate	–
		2:1		Precipitate (day 10)	–
	Linoleic acid	1:1	60	Yellow homogenous liquid	Hydrophobic
		1:5		Yellow homogenous liquid	Hydrophobic
		5:1		Solid	–
		2:1		Precipitate (day 10)	–

determination of the UV filters after DES-based DLLME extraction. Agilent ChemStation B.01.03 software was employed for data acquisition. The chromatographic separation of UV filters was carried out in a Zorbax Eclipse XDB-C18 (150 mm × 4.6 mm, 5 μm) column purchased to Agilent Technologies (Waldbronn, Germany).

2.3. Preparation of deep eutectic solvents

Different DESs were prepared employing the "stirring and heating" method [7]. This technique consists of mixing the components (HBA and HBD) and stirring them at a certain temperature until a clear and homogeneous liquid is obtained. DESs synthesis was considered successful when a clear homogeneous liquid was observed at room temperature. The prepared DESs combinations and their molar ratios are given in Table 1.

2.4. Characterization of deep eutectic solvents

Density measurements were carried out at 25 °C using the vibrating quartz U-tube Anton Paar DMA 5000 M density meter from Anton Paar (Graz, Austria). The same equipment was considered to determine the thermal expansion coefficient defined as $\alpha = -\rho^{-1}(\partial\rho/\partial T)_{p,c}$. Thermal expansion coefficient was calculated by measuring the density of DES at five different temperatures, starting from 1.0 °C below the working temperature (this work 25 °C) up to 1.0 °C above it, with an increment of 0.5 °C. $(\partial\rho/\partial T)$ was determined by a linear regression fit and ρ corresponds to the density of DESs at the average working temperature. An Abbemat Multiwavelength MW refractometer from Anton Paar (Graz, Austria) was used to determine the refractive index of DESs at 25 °C for seven different wavelengths (i.e., 435.8, 480.0, 514.5, 546.1, 589.3, 632.8 y 656.3 nm). An AMVn digital micro-viscosimeter from Anton Paar (Graz, Austria) was utilized to determine the dynamic viscosity at 25 °C and different predefined angles (40°, 50°, 60° and 70°). The micro-viscosimeter was equipped with a capillary of 1.8 mm (diameter), which was limited for mixtures with a dynamic viscosity range of 2.5–70 mPa·s. For DESs which exceeded this limit (containing TBAC), a Physica MCR 501 rheometer from Anton Paar (Graz, Austria) with parallel plates of 20 mm diameter was used to measure the viscosity at 25 °C. Thermal conductivity measurements of DESs at 25 °C were performed using a Transient Hot-Wire (THW-L1) conductimeter from Thermtest Instruments (Hanwell, Canada). A Sigma 701 Force Tensiometer from Biolin Scientific (Hängpilsgatan, Sweden) was employed to determine the surface tension of DESs at 25 °C with the Platinum Du Nouy ring. Ionic conductivity was measured using a GLP 31 conductimeter from Crison (Barcelona, Spain). Three independent measurements were performed for the determination of the properties of DESs in order to verify the obtained results.

FT-IR and ^{1}H NMR spectra were obtained to confirm the formation of the DESs. For this purpose, a Jasco FTIR 4100 Fourier transform infrared spectrometer (FT-IR) from Jasco Europe S.r.l. (Cremella, Italy) in the range of 800–4000 cm^{-1} and a Bruker Avance 500 NMR from Bruker (Vienna, Austria) were used. For the ^{1}H NMR experiments, the DESs and their individual components were dissolved in $CDCl_3$. The uncertainty of the ^{1}H NMR equipment was evaluated by measuring 10 replicates of thymol, giving a value of 0.002 ppm for the hydrogen of the hydroxyl group, which suffers the most variability. Thermal decomposition of DESs and their precursor components was performed by thermogravimetric analysis (TGA), using a Setsys evolution thermal analyser from Setaram (Caluire-et-Cuire, France). Around 20 mg of the sample were weighed, introduced in a glass capsule and heated from 30 to 500 °C, at a rate of 10 °C min^{-1}, under a N_2 flow of 20 mL min^{-1}.

2.5. Application of deep eutectic solvents to the extraction of UV filters from aqueous samples

The extraction of UV filters from water samples was carried out using a DLLME procedure. Briefly, 4 mL of the sample were transferred to a 15 mL Falcon™ tube and spiked with 200 ng mL^{-1} of target compounds. Then, 200 μL of DES were added into the tube and the mixture was stirred at 2250 rpm for 5 min, achieving the complete dispersion of the DES through the aqueous phase. Finally, it was centrifuged at 4000 rpm for 5 min at room temperature and the upper phase (DES with the analytes) was collected, transferred to a chromatographic vial and injected into the HPLC-VWD system.

The chromatographic separation was performed with a mobile phase consisted of solvent A (type I grade water, 1 % v/v acetic acid), solvent B (acetonitrile) and solvent C (isopropanol) by isocratic elution at a mixing ratio of 10.8:85:4.2 (v/v). The flow rate was set at 1 mL min^{-1} and the column temperature was kept constant at 25 °C. The detection wavelength was 300 nm and the run time was 10 min. The injection volume was 1 or 10 μL, depending on the DES, in order to avoid the matrix effect.

The developed DES-based DLLME-HPLC-VWD method fulfilled the criteria of the ICH harmonized guideline "validation of analytical procedures" Q2(R2) [33] and was applied to the analysis of UV filters from water samples using each characterized DES.

3. Results and discussion

3.1. Preparation and selection of hydrophobic deep eutectic solvents

Type III and type V DESs were prepared combining TBAC, ChCl or thymol as HBA and different carboxylic acids (acetic acid, oxalic acid, palmitic acid, stearic acid, oleic acid and linoleic acid) as HBD. Firstly, diverse DESs combinations at molar ratios of 1:1, 1:5 and 5:1 were prepared and their organoleptic stability was determined based on the visualization of phase-break or color change over time. Results are presented in Table 1. DESs that presented any change in their physical state, such as, precipitation or solidification, during the next days from their preparation were discarded for further experiments. This change in their physical state is an indication of the breakdown of the DES, proving its low stability. Based on these results, other molar ratios were investigated, depending on the DES combination, to establish the formation capacity of each DES mixture, and the same criteria was applied to determine their stability. Hence, DESs formation was considered successfully when a clear and homogeneous liquid was obtained at room temperature, presenting an organoleptic stability for one month. DES formation was considered prosperous for ChCl:oxaA (1:1), ChCl:oleA (1:5), TBAC:aceA (1:5), TBAC:palA (1:1, 5:1), TBAC:oleA (1:1, 1:5, 2:1), TBAC:linA (1:1, 1:5, 2:1), thymol:aceA (1:1, 5:1, 1:10), thymol:oleA (1:1, 1:5) and thymol:linA (1:1, 1:5) combinations. These prepared DESs were homogeneous liquids, without precipitates at ambient temperature.

The effect of temperature in DES preparation process was evaluated since it strongly influences the properties of DESs. At first, the preparation temperature was selected based on the melting points of the individual components. Essays showed mixtures with precipitates, indicating that the successful DES formation did not occur using the same preparation temperatures as the melting points of the substances. Therefore, higher temperatures than melting points were required for achieving the successful DES formation. The necessary temperatures to achieve the successful preparation of these DESs are shown in Table 1.

In summary, the optimization of the minimum temperature required is essential in DES preparation processes for achieving stable DESs combinations.

Finally, the hydrophobicity of these DESs was evaluated studying their behaviour in contact with water in order to determine their potential application to environmental water extraction (Table 1). As the

DESs combinations of ChCl:oxaA 1:1, ChCl:oleA 1:5, TBAC:aceA 1:5 and thymol:aceA 1:10 proved to be hydrophilic, they were discarded for further experiments since they were not suitable for the application of the extraction process in water samples. Moreover, the DESs that showed precipitation after their addition to the water, indicating a phase rupture and, thus their poor stability (TBAC:palA 1:1 and 5:1 and thymol:aceA 1:1 and 5:1) were also discarded. Therefore, the selected hydrophobic DESs combinations were TBAC:oleA 1:1 and 1:5, TBAC: linA 1:1, 1:5 and 2:1 (type III), thymol:oleA 1:1 and 1:5, and thymol:linA 1:1 and 1:5 (type V).

To our knowledge, the preparation and characterization of the DESs thymol:oleA 1:5, thymol:linA 1:1 and 1:5, TBAC:oleA 1:5 and TBAC:linA 1:1, 1:5 and 2:1 have not been described in bibliography, and the DESs thymol:oleA 1:1 and TBAC:oleA 1:1 will be applied for the first time to the extraction of UV filters [31,32]. All these DESs are not included in the database of the DESs prepared and described in bibliography [34].

3.2. Physicochemical characterization

Physicochemical characterization of DESs considered as viable (hydrophobic and stable over time) was carried out using different techniques to determine the properties of DESs and to prove the intermolecular interactions, as hydrogen bonds between components, in order to confirm the successful formation of the DESs.

3.2.1. ^1H NMR

^{1}H NMR was employed to explore the interactions between components of DESs. The ^{1}H NMR spectra of type III and V DESs are given in Supplementary Material, and Table 2 summarizes the most significant chemical shifts obtained for both types of DESs. The strength of the interactions created between HBAs and HBDs was assessed by comparing the chemical shifts of the individual components with those of the DESs, providing insights into the robustness of these interactions. Figs. S1-S13 show that DESs formation consisted of intermolecular interactions as new signals were not observed in the spectra of all the studied DESs, comparing with the individual components, thus concluding that there was no chemical interaction between the components. As it was reported by Florindo et al. [9], the most significant changes in chemical shifts and consequently, higher changes in chemical shift of protons ($\Delta\delta_H$) should be observed in the hydrogens next to the hydrogen bond formation.

In the case of type V DESs, significant signals of the individual components that should show chemical shifts after the formation of DESs were located at 4.62 ppm for the hydroxyl group of thymol, and 10.90 and 10.82 ppm for the carboxyl groups of oleic and linoleic acid, respectively (Figs. S1-S3). For these DESs (Figs. S4-S7), a slight shift was obtained in the hydroxyl group of thymol, which shifted from 4.62 ppm to 4.65 and 4.63 ppm in DESs formed with oleic acid in 1:1 and 1:5 molar ratios, respectively ($\Delta\delta_H = 0.03$ and 0.01). In the combination with linoleic acid the shifts were more evident, moving from 4.62 ppm to 4.67 and 3.67 ppm for 1:1 and 1:5 molar ratios ($\Delta\delta_H = 0.05$ and 1.00). Differences in chemical shifts were more noticeable in the DESs formed with linoleic acid, demonstrating a stronger interaction. This is evidenced by changes in the signals of carboxyl groups of oleic and linoleic acid, moving at high field from 10.90 ppm to 10.85 and 10.75 ppm with oleic acid 1:1 and 1:5 ($\Delta\delta_H = 0.05$ and 0.15), and from 10.82 to 10.58 and 10.48 ppm with linoleic acid 1:1 and 1:5 ($\Delta\delta_H = 0.24$ and 0.34). The increase of the concentration of the carboxylic acid increases the strength of the intermolecular interaction since changes in chemical shifts are more evident. Slight changes in chemical shifts of hydrogens and the non-formation of new signals demonstrate the successful DESs formation via intermolecular interactions, as a physical process. This phenomenon was previously evidenced by other authors [35–37].

Furthermore, the rise in $\Delta\delta_H$ of thymol in the presence of carboxylic acids suggests that protons of carboxylic acids own less shielded environment and greater acidity with decreasing the molar ratio of thymol. The value of $\Delta\delta_H$ is highly dependent on the protons position in each

Table 2
^{1}H NMR chemical shifts for type III and V DESs and their individual components.

Peak	δ individual compounds (ppm)			δ DESs (ppm)							
	HBA	Oleic acid	Linoleic acid	Thymol:oleA 1:1	Thymol:oleA 1:5	Thymol:linA 1:1	Thymol:linA 1:5	TBAC:oleA 1:1	TBAC:oleA 1:5	TBAC:linA 1:1	TBAC:linA 1:5	TBAC:linA 2:1
5 (Thymol)	4.62	–	–	4.65	4.63	4.67	3.67					
7 (OleA)	–	10.90	–	10.75	10.85	–	–	4.56	6.91	–	–	–
8 (LinA)	–	–	10.82	–	–	10.58	10.48	–	–	5.17	3.90	3.74
4 (TBAC)	3.40	–	–	–	–	–	–	3.35	3.34	3.34	3.37	3.38

molecule, presenting the hydroxyl proton the higher $\Delta\delta_H$ values as that is where the interaction takes place. Herein, the nuclei are less shielded from the applied magnetic field since the increased in hydrogen bonding removes the electron density from the local vicinity of the nucleus. Therefore, the formation of intermolecular hydrogen bonding in the DESs is pushed by the greater acidity of the hydroxyl proton, making carboxylic acids excellent HBDs [38].

In the case of type III DESs, the changes in chemical shifts were highlighted in methyl groups next to nitrogen of TBAC (located at 3.40 ppm in Fig. S8) and in the carboxyl groups of the carboxylic acids (i.e., oleic and linoleic acid). Figs. S9-S13, corresponding to type III DESs, showed that the chemical shift of these methyl groups in TBAC moved at high field from 3.40 ppm to 3.35 and 3.34 ppm using oleic acid as HBD for 1:1 and 1:5 molar ratios ($\Delta\delta_H = 0.05$ and 0.06) and to 3.34, 3.37 and 3.38 ppm using linoleic acid as HBD for 1:1, 1:5 and 2:1 molar ratios ($\Delta\delta_H = 0.06$, 0.03 and 0.02). Moreover, signals of carboxyl groups of oleic and linoleic acid moved significantly at high field from 10.90 ppm to 4.56 and 6.91 ppm with oleic acid 1:1 and 1:5 ($\Delta\delta_H = 6.34$ and 3.99) and from 10.82 ppm to 5.17, 3.90 and 3.74 ppm with linoleic acid 1:1, 1:5 and 2:1 ($\Delta\delta_H = 5.65$, 6.92 and 7.08). These significant changes in chemical shifts, especially observed in carboxylic acids, confirmed the formation of strong hydrogen bond interactions between HBAs and HBDs, proving the successful formation of highly stable DESs [31]. Concretely, in DESs composed of TBAC and oleic acid, as the concentration of oleic acid increased, the change in the chemical shift was smaller, hence the intermolecular hydrogen bond was weaker. By contrast, employing linoleic acid as HBD, the increase in linoleic acid concentration increased the strength of the hydrogen bond formed.

In this case, the rise in $\Delta\delta_H$ of TBAC in the presence of oleic acid suggests that protons of the carboxylic acid own less shielded environment and greater acidity with increasing the molar ratio of thymol. However, this effect is reversed in the DESs formed with linoleic acid as HBD. For type III DESs, the formation of intermolecular hydrogen bonding in the DESs is driven by the greater basicity of the near-nitrogen protons of the TBAC and the greater acidity of the hydroxyl proton of carboxylic acids, making TBAC and carboxylic acids excellent HBA and HBDs [38].

3.2.2. FT-IR

Figs. 2 and 3 present the FT-IR spectra of type V and III DESs studied and their individual components. Moreover, the FT-IR characteristic bands of the functional groups of type III and V DESs and their precursor components are summarized in Table 3.

Thymol showed stretching vibration bands at 3158 cm^{-1} (O–H), 2865 and 1949 cm^{-1} (symmetric and asymmetric $–CH_2$), 1584–1620 cm^{-1} (aromatic C=C) and 1239 cm^{-1} (C–O). The stretching vibrations bands present for oleic acid are 2459–3292 cm^{-1} (O–H), 2852 and 2921 cm^{-1} (symmetric and asymmetric $–CH_2$), 1708 cm^{-1} (C=O), 1408–1456 and 922 cm^{-1} (in plane and out of plane O–H) and 1283 cm^{-1} (C–O), and for linoleic acid 2462–3328 cm^{-1} (O–H), 2854 and 2923 cm^{-1} (symmetric and asymmetric $–CH_2$), 1707 cm^{-1} (C=O), 1457–1416 and 917 cm^{-1} (in plane and out of plane O–H) and 1281 cm^{-1} (C–O). The FT-IR spectra of the prepared DESs presented the same profiles, maintaining the characteristic bands of the precursors. As can be seen in Table 3, type V DESs exhibited a broadening of the O–H stretching vibration bands and slight shifts in some bands. The O–H broadenings were presented at 2436–3665, 2412–3587, 2379–3587 and 2427–3414 cm^{-1} for thymol:oleA 1:1, thymol:oleA 1:5, thymol:linA 1:1 and thymol:linA 1:5, respectively, evidencing the formation of hydrogen bonds between the components. This effect is produced by a reduction of the force constant caused by proton transfer through the hydrogen bonding of the components, leading to peak broadening [39]. Slight shifts were also observed in C-O bands to lower wavenumbers from 1282 cm^{-1} for oleic acid and from 1281 cm^{-1} for linoleic acid to 1223 and 1222 cm^{-1}, respectively, in all type V DESs. These shifts suggest an increase of the electron density of the carbonyl oxygen, which may be attributed to the formation of hydrogen bonds between components [40]. Hence, the O–H band broadenings and the wavenumber shifts in C-O bands indicated the formation of hydrogen bonds between thymol and fatty acids in the vicinity of the –COOH group, consequently, confirming the successful formation of DESs, as it was previously reported for thymol:oleA 1:1 DES [32].

The successful formation of TBAC:oleA and TBAC:linA DESs was also proved by FT-IR analysis studying their hydrogen bond formation. The TBAC presented stretching vibration bands at 2871 and 2956 cm^{-1}

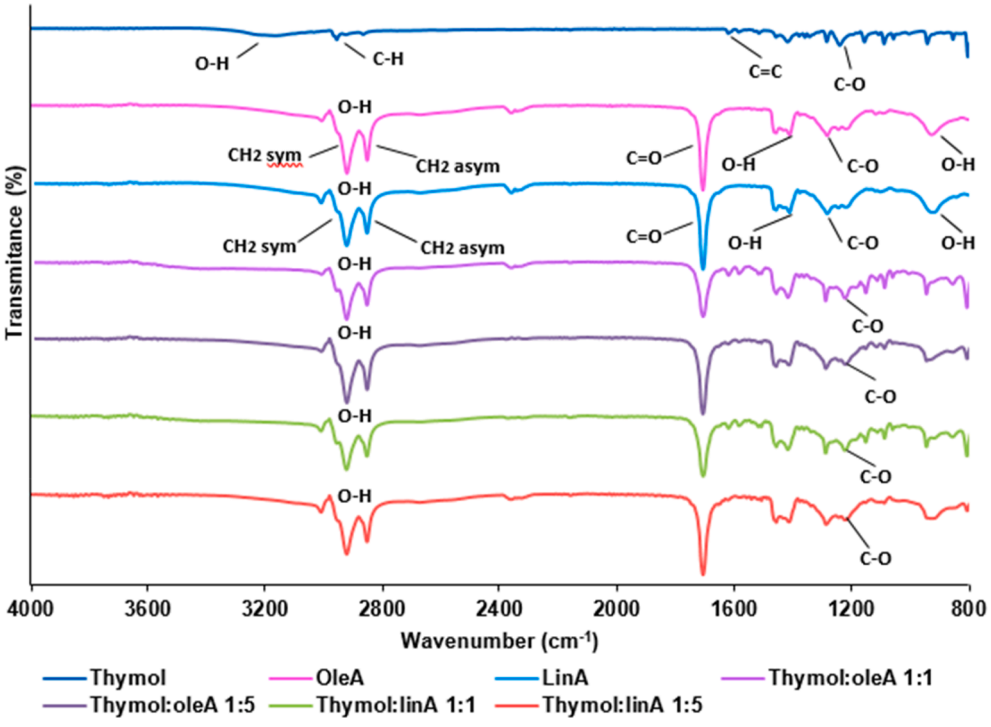

Fig. 2. FT-IR spectra of type V DESs and their individual components.

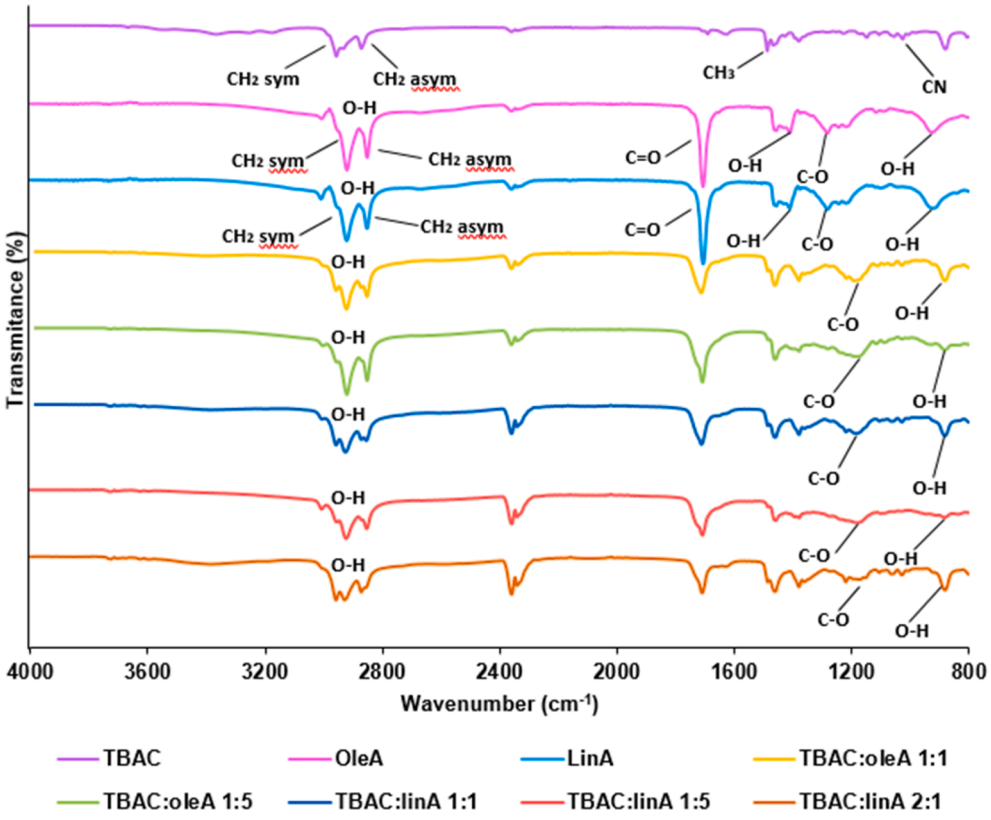

Fig. 3. FT-IR spectra of type III DESs and their individual components.

(symmetric and asymmetric –CH_2) and 1025 cm^{-1} (C-N). The peaks observed at 1466 and 1488 cm^{-1} correspond to the bending vibration of –CH_3 and the peaks at 3400 cm^{-1} could be a consequence of moisture during transport for analysis since TBAC is a hygroscopic substance [41]. In type III DESs, noticeable broadenings in the O–H stretching vibration bands (ranging from 2400 to 3600 cm^{-1}) were also observed, caused by the proton transfer through the hydrogen bonding of the components [39]. Likewise, the peak observed in oleic acid at 1408–1456 cm^{-1} (in plane O–H) disappeared in the DESs, and the peak at 1283 cm^{-1} (C-O) shifted to lower wavenumber in TBAC:oleA 1:1 and 1:5 DESs. In addition, the peak out of plane O–H shifted to lower wavenumber, from 922 cm^{-1} to 881 and 879 cm^{-1} in these DESs. These shifts suggest an increase of the electron density of the carbonyl oxygen, attributed to the formation of hydrogen bonds between components [40]. In linoleic acid-based type III DESs the same changes in bands were observed. The band at 1416-1457 cm^{-1} (in plane O–H) also disappeared, and the peaks at 1281 cm^{-1} (O–H) and 917 cm^{-1} (out of plane O–H) shifted to lower wavenumbers in TBAC:linA 1:1, 1:5 and 2:1 DESs. Therefore, as it happens in type V DESs, wavenumber shifts and O–H band broadenings evidenced the hydrogen bond formation between the precursor components, demonstrating the successful DESs preparation [42]. The hydrogen bond formation of the DES TBAC:oleA 1:1 was confirmed by Chen et al. [31].

The FT-IR spectra yielded conclusive evidence, demonstrating the occurrence of intermolecular interactions between the starting reagents employed in the preparation of the eutectic solvents. Variations in properties of DESs is attributed to the number of hydrogen bonds formed between HBAs and HBDs. More availability of hydroxyl groups (–OH) in components leads to an increase in the number of hydrogen bonds formed among them [43].

3.2.3. *Density and thermal expansion coefficient*

Densities of hydrophobic DESs were determined at room temperature. Variations in densities can be explained upon the basis of the Hole Theory [44], which describes that the difference of densities between different HBA and HBD combinations are attributed to a different molecular organization of DESs. According to this theory, DESs are composed of holes and during the combination of different HBAs and HBDs, the hole average sizes change, and thus the density value of the DES. Therefore, the difference in densities between different HBA and HBD combinations is attributed to a different molecular organization or packing of the DES. The principal factor that leads to DESs formation is the hydrogen bonding between the components, thus density values change depending on the strength of this bonding which is influenced by the DES components (different alkyl chain length or ion type) and their molar ratios [17]. Moreover, a higher number of hydrogen bonds reduce the free spaces available and, consequently, increase the density of DESs [16,44]. As it is observed in Table 4, DESs presented a decrease in density values with increasing the molar ratio of HBD due to increase in free volume [45], and all the studied DESs owned densities lower than water. This property is crucial since the liquid–liquid extraction methods usually require the collection of the DES phase (containing the analytes) after centrifugation, and this way the DES remains in the upper phase facilitating its collection. Density values of DESs were lower than those of their precursor HBAs (ρ_{thymol} = 0.965 g·cm^{-3} and ρ_{TBAC} = 1.018 g·cm^{-3}) and similar to those of their precursor HBDs (ρ_{oleA} = 0.895 g·cm^{-3} and ρ_{linA} = 0.900 g·cm^{-3}). This variation might be attributed to changes in the average hole sizes during the formation of DESs, prevailing the density of the HBDs. Garcia et al. reported that most of the reported type III DESs densities are higher than water, ranging from 1 to 1.35 g·cm^{-3} [46]. In addition, DESs based on metals salts presented densities between 1.3 and 1.6 g·cm^{-3}, whereas, hydrophobic DESs (those studied in this work) obtained densities lower than water [26,47,48].

Thermal expansion coefficient is a unique property for each fluid and measures the tendency of a fluid to expand when heated and to contract when cooled. Thermal expansion coefficient describes the change in volume of a liquid with temperature, indicating the free volume of

Table 3
FT-IR characteristic bands of type III and type V DESs and their precursor components.

Band	Wavenumber (cm^{-1})										
	HBA	OleA	LinA	Thymol:oleA 1:1	Thymol:oleA 1:5	Thymol:linA 1:1	Thymol:linA 1:5	TBAC:oleA 1:1	TBAC:oleA 1:5	TBAC:linA 1:1	TBAC:linA 1:5	TBAC:linA 2:1
$\nu_{C\text{-}N}$	1025	–	–	–	–	–	–	–	–	–	–	–
$\nu_{C=C}$	1584–1620	–	–	1583–1617	–	1521–1618	–	–	–	–	–	–
$\nu_{O\text{-}H}$	–	2459–3292	2462–3328	2436–3665	2412–3587	2379–3587	2427–3414	2400–3600	2400–3600	2400–3600	2400–3600	2400–3600
$\nu_{CH2\ sym}$	2864	2852	2854	2853	2852	2852	2853	2853	2853	2852	2854	2872
$\nu_{CH2\ asym}$	2949	2921	2923	2923	2921	2920	2920	2922	2922	2926	2923	2928
$\nu_{C=O}$	–	1708	1707	1703	1707	1703	1706	1713	1709	1712	1709	1709
$\nu_{O\text{-}H\ in\ plane}$	–	1456	1457	1455	1455	1456	1457	–	–	–	–	–
$\nu_{C\text{-}O}$	1239	1283	1281	1223	1221	1222	1217	1179	1174	1177	1177	1175
$\nu_{O\text{-}H\ out\ of\ plane}$	–	922	917	–	–	–	–	881	879	882	880	880

solvents. In other words, higher thermal expansion coefficient values correspond to higher free volumes that create additional spaces between unbound molecules, thus decreasing the density. The estimated thermal expansion coefficient values are presented in Table 4 and ranged from $6.56{\cdot}10^{-4}$ to $7.85{\cdot}10^{-4}$ K^{-1}. In general, the thermal expansion coefficient values were high compared to previous studies, which explains the obtained lower density values compared to other DESs [49]. The addition of HBD increases the thermal expansion coefficient in type III DESs. This is probably due to a decrease of hydrogen bond interactions between the components, which results in a decrease in density, a higher free volume and, consequently, an increase in the thermal expansion coefficient. The opposite effect was observed in type V DESs. However, as the variation in thermal expansion coefficients was minimal in this type of DESs, it can be concluded that temperature and molar ratio did not significantly affect their thermal expansion coefficient.

3.2.4. Refractive index

Refractive index is an important optical property of materials calculated from the ratio of the speed of light in vacuum to that in a second medium. Nonetheless, its determination remains limited in the field of DESs.

Fig. 4 presents a decrease in refractive index when increasing the wavelength since different wavelengths interfere to different extents with the atoms of the medium. The refractive index of DESs at 589.3 nm shown in Table 4 ranged from 1.461 to 1.478 and did not show significant differences with those of the individual components ($n_{oleA} = 1.458$ and $n_{linA} = 1.466$). According to literature, DESs commonly exhibit refractive index values between 1.43 and 1.56, showing higher values than water (1.33), since molecules with larger sizes have higher refractive index [20,34]. These higher refractive index values of DESs might have influenced in a better phase separation after the centrifugation of the DLLME process.

In both type of DESs the refractive index values decreased by increasing the molar ratio of the HBD. The addition of more HBD, which acts as a solvent, was added into the solution containing the HBA (solute) resulting in a less concentrated solution. This means that less light strikes the molecules, thus reducing the refractive index [34].

3.2.5. Surface tension

Surface tension is a crucial property for DES characterization since it is highly dependent on the strength of the intermolecular interactions between the HBA and HBD, temperature, molar ratio, nature of HBAs/HBDs and the alkyl chain length [20]. Hence, liquids of high density and viscosity present high surface tensions.

As can be observed in Table 4, the DESs studied in this work presented surface tensions concordant to bibliography in a range of 31.6–33.4 $mN{\cdot}m^{-1}$, which generally show values between 30 and 60 $mN{\cdot}m^{-1}$ at 25 °C [34]. This property could help the phase separation employing the DLLME procedure in water samples due to the difference in surface tension of the DESs with water ($\gamma_{water} = 72.8$ $mN{\cdot}m^{-1}$).

Surface tensions were practically not influenced by the formation of DESs as the surface tensions of oleic acid and linoleic acid were 31.9 and 30.4 $mN{\cdot}m^{-1}$, being similar to those of DESs. The surface tension decreased or increased slightly together with the molar ratio of the HBD, depending on the nature of the HBA. In type V DESs, the change in surface tension was not significant (31.6, 31.7, 31.9 and 32.1 $mN{\cdot}m^{-1}$ for thymol:oleA 1:1 and 1:5 and thymol:linA 1:1 and 1:5). Type III DESs showed a more evident decrease in surface tension with increasing the molar ratio of the HBD (32.9, 31.6, 33.4, 32.8 and 32.0 $mN{\cdot}m^{-1}$ for TBAC:oleA 1:1 and 1:5 and TBAC:linA 2:1, 1:1 and 1:5). No significant differences were observed in surface tension values using oleic or linoleic acid as HBD.

The effect of the components and molar ratio on surface tension may be explained by the Hole theory, which describes the relationship between surface tension and the average hole size. Based on this theory, higher proportion of larger holes results in lower surface tension of a

Table 4
Prepared type III and V DESs and their physicochemical properties (density (ρ), thermal expansion coefficient (α), refractive index (*n*), surface tension (γ), dynamic viscosity (μ), ionic conductivity (κ) and thermal conductivity (λ)) at 25 °C.

DES	ρ (g·cm^{-3})	α · 10^{-4} (K^{-1})	*n* at 589.3 nm	γ (mN·m^{-1})	μ (mPa·s)	κ (S·m^{-1})	λ (W·m^{-1}K^{-1})
Thymol:oleA 1:1	0.913	7.85	1.478	31.6	23.4	0.04	0.152
Thymol:oleA 1:5	0.895	7.74	1.464	31.7	27.1	0.36	0.160
Thymol:linA 1:1	0.914	7.81	1.478	31.9	20.5	0.28	0.154
Thymol:linA 1:5	0.901	7.75	1.468	32.1	21.9	1.34	0.160
TBAC:oleA 1:1	0.911	6.66	1.471	32.9	460.6	63.6	0.153
TBAC:oleA 1:5	0.893	7.32	1.461	31.6	85.6	13.9	0.158
TBAC:linA 2:1	0.918	6.56	1.475	33.4	535.5	82.3	0.152
TBAC:linA 1:1	0.911	6.83	1.471	32.8	221.0	77.4	0.153
TBAC:linA 1:5	0.900	7.36	1.466	32.0	57.0	13.1	0.159

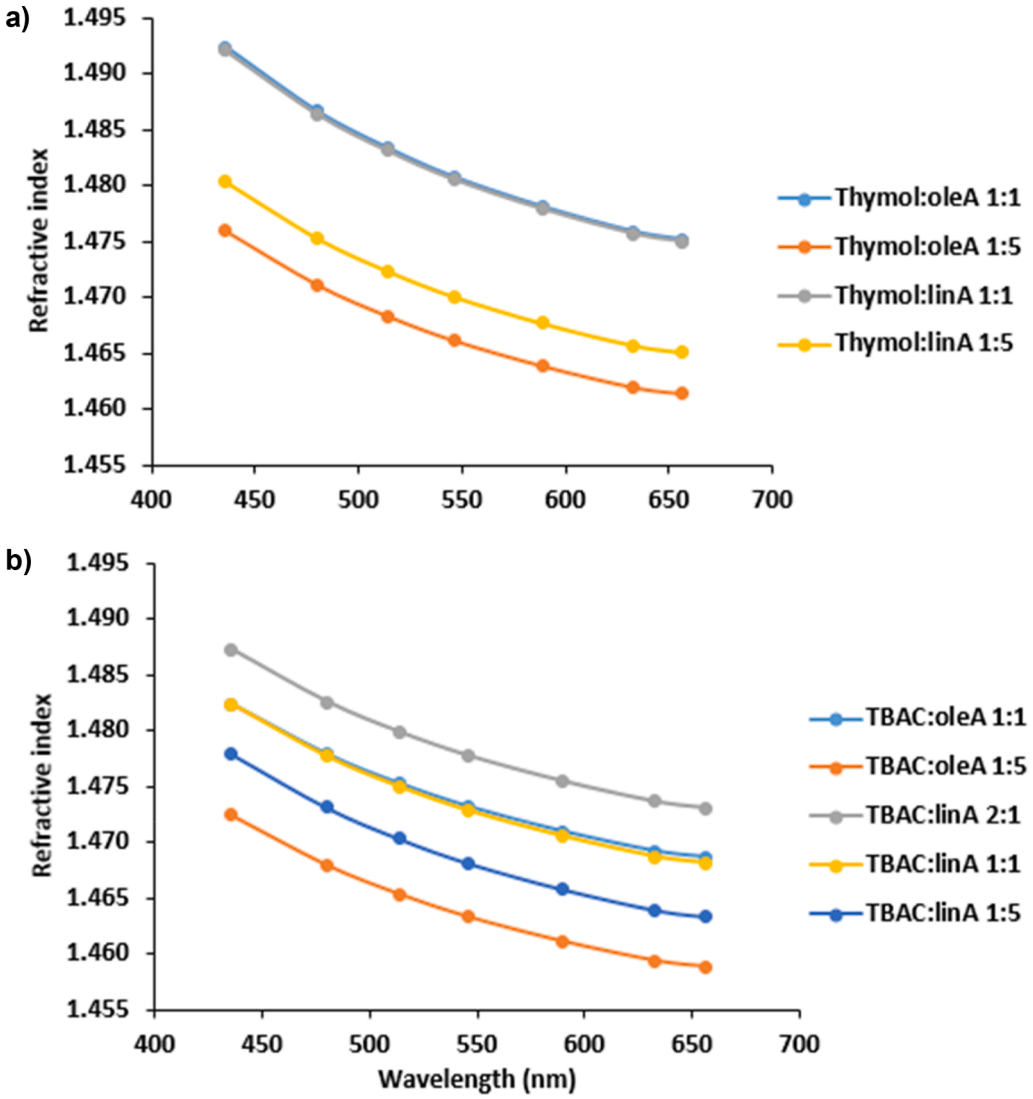

Fig. 4. Refractive index at different wavelengths for a) type V and b) type III DESs at 25 °C.

liquid since the free volume increases by decreasing the ionic interactions [45].

3.2.6. *Viscosity*

Viscosity is an important physical property of DESs since the applicability of a solvent as a reaction media usually is decided considering the viscosity of the solvent. The presence of an extensive hydrogen bond network between the components of DESs is the main cause of their high viscosities since it reduces the movement of free species in the DESs [44]. Other factors related with the high viscosities of DESs are Van der Waals or electrostatic interactions, the size of ions and the available free volume [21]. The viscosities of DESs are affected by the chemical nature of HBAs and HBDs, temperature, molar mass, and the molar ratio [25].

Most of the studied DESs have been recognized as viscous liquids at room temperature presenting higher viscosities than water which is 1 mPa·s [16]. As it is shown in Table 4, the prepared type III and V DESs also presented higher viscosities than water. This difference in viscosities between the DESs and water leads to a better phase separation

during the application of the DLLME procedure in water samples.

Overall, the viscosities of DES were very similar to those of their HBDs ($\mu_{oleA} = 31.9$ mPa·s and $\mu_{linA} = 26.7$ mPa·s), with the viscosity of the HBD prevailing in the DESs. Hence, the viscosity values of the studied DESs were mainly affected by the chemical structure of HBA. The DESs composed of TBAC obtained higher viscosities than those composed of thymol. This may be attributed to the different intermolecular hydrogen bond network depending on the components. Some studies suggested that the molecular structure of the components (i.e., molecular weight and size) could considerably affect the mobility of the whole system, increasing the viscosities [50]. In this case, TBAC presents higher molecular weight than thymol ($MW_{TBAC} = 277.9$ g·mol^{-1} and $MW_{thymol} = 150.2$ g·mol^{-1}) which significantly influenced the viscosity of DESs, obtaining a viscosity value of 535.5 mPa·s with the DES with the highest TBAC content (TBAC:linA 2:1). Likewise, the molar ratio affected the viscosities of type III and V DESs differently. In the case of type V DESs, viscosity values increased by decreasing the molar ratio of thymol. This behaviour may be attributed to the ability of thymol to disrupt the intermolecular hydrogen bonding of the HBD's structure, which led to a higher degree of freedom and, thus decreasing the viscosity of the DESs. However, for type III DESs, the increase in the molar ratio of HBD decreased the viscosity of the DES. This is because TBAC may act as a bridge connecting the other groups and, therefore, a lower molar ratio of HBA in DES causes a decrease in viscosity due to the poor network formed between the different groups of the HBA and HBD [34].

3.2.7. Ionic conductivity

Ionic conductivity is a significant characteristic for DESs since numerous investigations involve power system applications as their potential use in advanced electrolytes for redox-flow batteries [51]. Ionic conductivity is proportional to the rate of migration of ions inside the DESs and is directly proportional to the viscosity which is related to the Hole theory [44].

According to literature, due to relatively high viscosities of DESs they usually exhibit low conductivities (<1000 μS·cm^{-1}), as shown in Table 4 [34]. The DESs components and their molar ratios influenced the conductivity values of DESs. Ionic conductivities of type III DESs were higher than those of type V DESs as higher weight ratio of the TBAC in structure of DESs leads to higher conductivity values [34].

In type III DESs, by increasing the molar ratio of HBD, the amount of ions from HBA decreased, thus decreasing the ionic conductivity value of the mixture. Meanwhile, the ionic conductivities of type V DESs, whose viscosities increased by increasing the molar ratio of HBD, increased by addition of the HBD. This proves that ion mobility and, thus ionic conductivity are dependent not only on the availability of suitable voids, but also on the type and strength of HBA-HBD interactions [52].

3.2.8. Thermal conductivity

Thermal conductivity is essential for the application of DESs in heat transfer operations [53]. Nevertheless, although conventional properties of DESs have widely been investigated, the reported data about thermal conductivity are very scarce and mostly limited to ChCl-based DESs [54]. As can be seen in Table 4, thermal conductivity values did not show significant differences between type III and V DESs and ranged from 0.152 to 0.160 W·m^{-1} K^{-1}.

Results are in accordance with literature as previous studies demonstrated that large changes in thermal conductivity are only obtained when structurally very different HBAs and HBDs are involved (e.g., $\lambda_{ChCl:urea\ 1:2} = 0.245$ W·m^{-1} K^{-1}). Furthermore, these results presented negligible effect of molar ratios on thermal conductivity, since when the HBD content increased, the DESs presented practically the same thermal conductivity.

3.2.9. TGA

The evaluation of thermal stability of DESs is essential since it allows the determination of decomposition or phase changes of the solvent. In addition, it is possible to define the maximum temperature (T_{onset}) at which DESs maintain the liquid state without suffering alterations. The thermograms obtained are shown in Fig. 5 and in Table 5 onset temperatures are given.

As can be observed in Table 5, the values of the onset temperatures for the DESs are between those of their pure constituents, denoting a similar maximum working temperature. The only exception is the TBAC:linA 1:5 DES, being the value of its onset temperature higher than those of its pure components. In addition, thermograms showed that all the DESs and their precursor components were completely degraded in the temperature range of 170–400 °C.

Fig. 5a and 5b show the thermograms obtained for type V DESs and their precursors. The mass loss for thymol occurred at 170 °C, otherwise for oleic acid at 270 °C and for linoleic acid at 266 °C, according to the degradation temperature of the components. The thermal decomposition of oleic acid-based type V DESs (Fig. 5a) occurred in various steps, attributed to the decomposition of thymol and oleic acid. The thermal decomposition of thymol:oleA 1:1 and 1:5 occurred with a first mass loss of 28 % and 12 % at 175 °C and 176 °C, due to the removal of thymol. A second mass loss of 72 % and 88 % was determined at 248 °C and 260 °C attributed to the oleic acid. For linoleic acid-based type V DESs the same effect was observed (Fig. 5b). A first mass loss of 37 % and 15 % at 170 °C and 171 °C corresponding to thymol was observed for thymol:linA 1:1 and 1:5 DESs. The second mass loss 63 % and 85 % occurred at 258 °C and 262 °C, attributed to the linoleic acid.

In the case of type III DESs, the thermogram of TBAC (Fig. 5c and 5d) presented a 12 % of mass loss at around 100 °C due to the removal of water since this product contained < 7 % of water and TBAC is a hygroscopic substance. Complete thermal decomposition of TBAC occurred at 190 °C. The water content was 3 % for the DESs TBAC:oleA 1:1, 1:5 and TBAC:linA 1:5, and 7 % for TBAC:linA 1:1 and 2:1. As it was demonstrated with type V DESs, the thermal decomposition of these DESs also occurred in various steps, being characteristic of TBAC and each fatty acid. For TBAC:oleA 1:1 and 1:5 DESs, a first mass loss of 42 % and 30 % was determined at 213 °C and 222 °C due to the removal of TBAC. A second mass loss of 58 % and 70 % was defined at 262 °C and 265 °C, attributed to the oleic acid. For linoleic acid-based DESs, the first mass loss of 58 %, 24 % and 77 % were observed at 226 °C, 225 °C and 195 °C in 1:1, 1:5 and 2:1 molar ratios. The second mass loss corresponding to linoleic acid were of 42 %, 76 % and 23 % at 264 °C, 278 °C and 262 °C.

As can be seen, the difference in degradation percentages clearly varies with the molar ratio of the DESs. That is, as the molar ratio of the HBD increases, the degradation temperature its closer to that of its HBD, which is higher than that of the HBAs. Therefore, it is necessary to increase the proportion of the compound that has higher degradation temperatures in order to obtain higher thermally stable DESs.

These results evidenced that the degradation behaviour of DESs is highly dependent on the nature of the DES constituents and molar ratios [55]. The thermograms of the DESs are influenced by multiple factors that are involved in their formation and, thus their thermal properties. Hence, the nature of the HBA or HBD, intermolecular interactions, water composition, the number of carbon atoms and hydrogen bonding strength can highly affect the thermal stability of the DESs [40].

3.3. Application of deep eutectic solvents to the extraction of UV filters from aqueous samples

Hydrophobic DESs were evaluated for the extraction of three UV filters with different polarities (namely, BZ3, MBC, and OC) from aqueous samples using a validated DES-based DLLME-HPLC-VWD methodology.

The obtained %ERs for each UV filter after the DES-based DLLME-HPLC-VWD method are summarized in Table 6. The DESs composed of thymol and oleic acid provided the highest %ERs for all the UV filters evaluated, ranging from 99 % to 103 %. These high %ERs may be

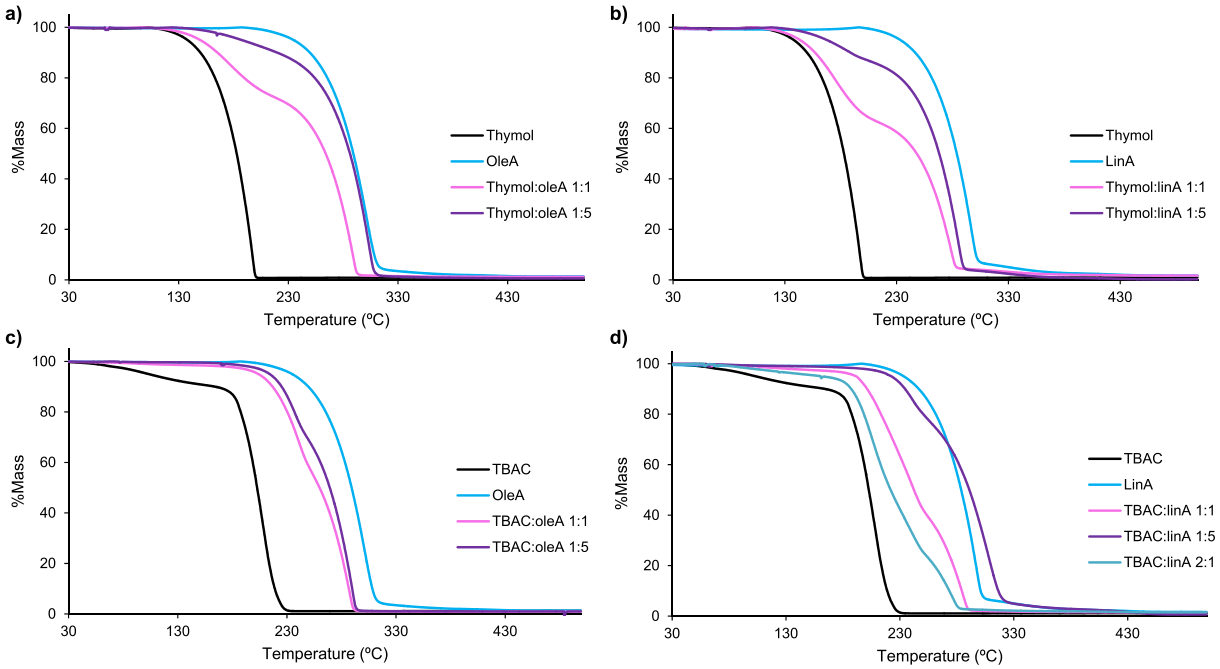

Fig. 5. TGA analysis of a) oleic acid-based type V DESs, b) linoleic acid-based type V DESs, c) oleic acid-based type III DESs and d) linoleic acid-based type III DESs.

Table 5
Onset decomposition temperatures and mass loss percentages of type III and type V DESs and their precursor constituents.

DESs	T_{onset} (°C)			Mass loss
	HBA	HBD	DES	DES
Thymol:oleA 1:1	170	270	175, 248	28 %, 72 %
Thymol:oleA 1:5	170	270	176, 260	12 %, 88 %
Thymol:linA 1:1	170	266	170, 258	37 %, 63 %
Thymol:linA 1:5	170	266	171, 262	15 %, 85 %
TBAC:oleA 1:1	190	270	213, 262	42 %, 58 %
TBAC:oleA 1:5	190	270	222, 265	30 %, 70 %
TBAC:linA 1:1	190	266	226, 264	58 %, 42 %
TBAC:linA 1:5	190	266	225, 278	24 %, 76 %
TBAC:linA 2:1	190	266	195, 262	77 %, 23 %

Table 6
Extraction recoveries (%ERs) obtained with different DESs combinations in Mili-Q water spiked at a concentration of 200 ng mL^{-1} for all the UV filters (%RSD of three replicates).

DES	BZ3	MBC	OC
Thymol:oleA 1:1	99 (3)	102 (1)	102 (1)
Thymol:oleA 1:5	103 (1)	101 (1)	102 (1)
Thymol:linA 1:1	n.d.	91 (1)	n.d.
Thymol:linA 1:5	n.d.	86 (2)	n.d.
TBAC:oleA 1:1	61 (4)	103 (1)	106 (2)
TBAC:oleA 1:5	103 (1)	97 (1)	76 (3)
TBAC:linA 1:1	n.d.	88 (1)	n.d.
TBAC:linA 1:5	n.d.	52 (2)	n.d.
TBAC:linA 2:1	n.d.	92 (1)	n.d.

n.d.: non-detected.

attributed to the formed London dispersion forces between the non-polar compounds (UV filters) and the hydrophobic solvent (thymol and oleic acid) [56]. Moreover, thymol could be able to establish π-π interactions with UV filters due to its aromaticity. Likewise, the UV filter with a log k_{ow} value of 5.14 (i.e., MBC) presented high %ERs (>88 %) in all cases except for the TBAC:linA 1:5 DES with only 52 %. This behaviour can be due to the effect of increasing the molar ratio of linoleic acid to TBAC, which leads to a decrease in the extraction capacity of the DES. Specifically, the extraction capacity decreased significantly from 88 % to 52 % as the TBAC:linA molar ratio increased from 1:1 to 1:5. This may be a consequence of the capacity of linoleic acid to form different conformations, such as lipid bilayers, as the molar concentration of linoleic acid increases. Hence, the excess of linoleic acid in 1:5 molar ratios could lead to a lower solubilization of UV filters in the DES, decreasing their %ER. All the resultant %RSD values were lower than 5 %, demonstrating the good repeatability of the proposed DES-based DLLME-HPLC-VWD method.

4. Conclusions

Hydrophobic type III and type V DESs based on carboxylic acids combined with TBAC or thymol as HBA have been successfully prepared and characterized. The DESs TBAC:oleA 1:5, TBAC: linA 1:1, 1:5 and 2:1, thymol:oleA 1:5, and thymol:linA 1:1 and 1:5 have been investigated for the first time as eutectic mixtures. The DESs formation via hydrogen bonding between components was clearly demonstrated in all cases since O–H band broadenings and band shifts were evidenced via FT-IR in all the DESs, and chemical shifts were also proved via ^{1}H NMR, being more evident in type III DESs.

Densities of DESs proved to be lower than water, facilitating the collection of the upper phase in liquid–liquid extractions, which contains the extractant (i.e., DESs) together with the analytes. Furthermore, the resultant refractive index, surface tension and dynamic viscosity values of DESs were different than those of water. This difference contributed to improved phase separation in the liquid–liquid extraction.

The onset decomposition temperature values were determined for each DES and the precursor components, defining the thermal behaviour of the DESs, generally being in the ranges of the individual constituents.

Moreover, these type III and type V DESs demonstrated ability as UV filter extractants from aqueous samples. The DESs consisted of thymol and oleic acid provided the highest %ERs ranging from 99 % to 103 %, suggesting the high compatibility between the components of the DESs and the UV filters.

On balance, all these results showed the potential applicability of these novel DESs to the analysis of pollutants from environmental waters inside a green chemistry framework.

CRediT authorship contribution statement

Alaine Duque: Investigation, Writing – original draft. **Antton Sanjuan:** Investigation. **M. Mounir Bou-Ali:** Supervision, Methodology, Funding acquisition. **Rosa M. Alonso:** Conceptualization, Supervision, Methodology, Funding acquisition, Writing – review & editing. **Miguel A. Campanero:** Conceptualization, Supervision, Methodology, Funding acquisition, Writing – review & editing.

Declaration of Competing Interest

The authors declare that they have no known competing financial interests or personal relationships that could have appeared to influence the work reported in this paper.

Data availability

Data will be made available on request.

Acknowledgements

Authors thank Jose Ignacio Gutierrez Ortiz from Chemical Technologies for Environmental Sustainability Group from the University of Basque Country (UPV/EHU), for his help for carrying out the thermogravimetric and DSC measurements.

A.D. thanks the Basque Country Government for her predoctoral contract (Bikaintek 2020 Program from the Regional Minister for Economic Development and Infrastructures (order 2021–1353, file number 021-B2/2020)). R.M.A thanks the Education Department of Basque Country Government for financial support (project IT1673-22). A.S. wants to thank the Basque Government for funding under an FPI grant (PRE_2022_1_0136). M.M.B would like to thank the financial support from the Basque Government under the Research Group Programme IT1505-22 and μ4Smart KK-2023/00016.

Appendix A. Supplementary data

Supplementary data to this article can be found online at https://doi.org/10.1016/j.molliq.2023.123431.

References

[1] Á. Santana-Mayor, R. Rodríguez-Ramos, A.V. Herrera-Herrera, B. Socas-Rodríguez, M.Á. Rodríguez-Delgado, Deep eutectic solvents. The new generation of green solvents in analytical chemistry, TrAC - Trends in Analytical Chemistry 134 (2021), https://doi.org/10.1016/j.trac.2020.116108.

[2] A. Shishov, A. Pochivalov, L. Nugbienyo, V. Andruch, A. Bulatov, Deep eutectic solvents are not only effective extractants, TrAC - Trends Anal. Chem. 129 (2020) 115956, https://doi.org/10.1016/j.trac.2020.115956.

[3] S.C. Cunha, J.O. Fernandes, Extraction techniques with deep eutectic solvents, TrAC - Trends in Analytical Chemistry 105 (2018) 225–239, https://doi.org/10.1016/j.trac.2018.05.001.

[4] A.R.C. Duarte, A.S.D. Ferreira, S. Barreiros, E. Cabrita, R.L. Reis, A. Paiva, A comparison between pure active pharmaceutical ingredients and therapeutic deep eutectic solvents: Solubility and permeability studies, Eur. J. Pharm. Biopharm. 114 (2017) 296–304, https://doi.org/10.1016/j.ejpb.2017.02.003.

[5] S. Xia, G.A. Baker, H. Li, S. Ravula, H. Zhao, Aqueous ionic liquids and deep eutectic solvents for cellulosic biomass pretreatment and saccharification, RSC Adv. 4 (2014) 10586–10596, https://doi.org/10.1039/c3ra46149a.

[6] M.H. Zainal-Abidin, M. Hayyan, G.C. Ngoh, W.F. Wong, C.Y. Looi, Emerging frontiers of deep eutectic solvents in drug discovery and drug delivery systems, J. Control. Release 316 (2019) 168–195, https://doi.org/10.1016/j.jconrel.2019.09.019.

[7] A.P. Abbott, G. Capper, D.L. Davies, R.K. Rasheed, V. Tambyrajah, Novel solvent properties of choline chloride/urea mixtures, Chem. Commun. (2003) 70–71, https://doi.org/10.1039/b210714g.

[8] Y. Dai, G.J. Witkamp, R. Verpoorte, Y.H. Choi, Natural deep eutectic solvents as a new extraction media for phenolic metabolites in carthamus tinctorius L, Anal. Chem. 85 (2013) 6272–6278, https://doi.org/10.1021/ac400432p.

[9] C. Florindo, F.S. Oliveira, L.P.N. Rebelo, A.M. Fernandes, I.M. Marrucho, Insights into the synthesis and properties of deep eutectic solvents based on cholinium chloride and carboxylic acids, ACS Sustainable Chemistry & Engineering 2 (2014) 2416–2425, https://doi.org/10.1021/sc500439w.

[10] M.C. Gutiérrez, M.L. Ferrer, C.R. Mateo, F. Del Monte, Freeze-drying of aqueous solutions of deep eutectic solvents: A suitable approach to deep eutectic suspensions of self-assembled structures, Langmuir 25 (2009) 5509–5515, https://doi.org/10.1021/la900552b.

[11] D.E. Crawford, L.A. Wright, S.L. James, A.P. Abbott, Efficient continuous synthesis of high purity deep eutectic solvents by twin screw extrusion, Chem. Commun. 52 (2016) 4215–4218, https://doi.org/10.1039/c5cc09685e.

[12] F.J.V. Gomez, M. Espino, M.A. Fernández, M.F. Silva, A greener approach to prepare natural deep eutectic solvents, ChemistrySelect 3 (2018) 6122–6125, https://doi.org/10.1002/slct.201800713.

[13] S. Bajkacz, J. Adamek, Development of a method based on natural deep eutectic solvents for extraction of flavonoids from food samples, Food Anal. Methods 11 (2018) 1330–1344, https://doi.org/10.1007/s12161-017-1118-5.

[14] S. Chakraborty, J.H. Chormale, A.K. Bansal, Deep eutectic systems: An overview of fundamental aspects, current understanding and drug delivery applications, Int. J. Pharm. 610 (2021) 121203, https://doi.org/10.1016/j.ijpharm.2021.121203.

[15] M.Q. Farooq, N.M. Abbasi, J.L. Anderson, Deep eutectic solvents in separations: Methods of preparation, polarity, and applications in extractions and capillary electrochromatography, J. Chromatogr. A 1633 (2020) 461613, https://doi.org/10.1016/j.chroma.2020.461613.

[16] S.P. Ijardar, V. Singh, R.L. Gardas, Revisiting the physicochemical properties and applications of deep eutectic solvents, Molecules 27 (2022) 1368, https://doi.org/10.3390/molecules27041368.

[17] T. El Achkar, H. Greige-Gerges, S. Fourmentin, Basics and properties of deep eutectic solvents: A review, Environ. Chem. Lett. 19 (2021) 3397–3408, https://doi.org/10.1007/s10311-021-01225-8.

[18] D.O. Abranches, M.A.R. Martins, L.P. Silva, N. Schaeffer, S.P. Pinho, J.A. P. Coutinho, Phenolic hydrogen bond donors in the formation of non-ionic deep eutectic solvents: The quest for type v des, Chem. Commun. 55 (2019) 10253–10256, https://doi.org/10.1039/c9cc04846d.

[19] D.O. Abranches, J.A.P. Coutinho, Type V deep eutectic solvents : Design and applications, Curr. Opin. Green Sustain. Chem. 35 (2022) 100612, https://doi.org/10.1016/j.cogsc.2022.100612.

[20] K.A. Omar, R. Sadeghi, Physicochemical properties of deep eutectic solvents: A review, J. Mol. Liq. 360 (2022) 119524, https://doi.org/10.1016/j.molliq.2022.119524.

[21] B.B. Hansen, S. Spittle, B. Chen, D. Poe, Y. Zhang, J.M. Klein, A. Horton, L. Adhikari, T. Zelovich, B.W. Doherty, B. Gurkan, E.J. Maginn, A. Ragauskas, M. Dadmun, T.A. Zawodzinski, G.A. Baker, M.E. Tuckerman, R.F. Savinell, J. R. Sangoro, Deep eutectic solvents: A review of fundamentals and applications, Chem. Rev. 121 (2021) 1232–1285, https://doi.org/10.1021/acs.chemrev.0c00385.

[22] H. Wang, S. Liu, Y. Zhao, J. Wang, Z. Yu, Insights into the hydrogen bond interactions in deep eutectic solvents composed of choline chloride and polyols, ACS Sustain. Chem. Eng. 7 (2019) 7760–7767, https://doi.org/10.1021/acssuschemeng.8b06676.

[23] N. Schaeffer, M.A.R. Martins, C.M.S.S. Neves, S.P. Pinho, J.A.P. Coutinho, Sustainable hydrophobic terpene-based eutectic solvents for the extraction and separation of metals, Chem. Commun. 54 (2018) 8104–8107, https://doi.org/10.1039/c8cc04152k.

[24] P. Makoś, A. Przyjazny, G. Boczkaj, Hydrophobic deep eutectic solvents as “green” extraction media for polycyclic aromatic hydrocarbons in aqueous samples, J. Chromatogr. A 1570 (2018) 28–37, https://doi.org/10.1016/j.chroma.2018.07.070.

[25] Q. Zhang, K. De Oliveira Vigier, S. Royer, F. Jérôme, Deep eutectic solvents: Syntheses, properties and applications, Chem. Soc. Rev. 41 (2012) 7108–7146, https://doi.org/10.1039/c2cs35178a.

[26] M.A.R. Martins, E.A. Crespo, P.V.A. Pontes, L.P. Silva, M. Bülow, G.J. Maximo, E.A. C. Batista, C. Held, S.P. Pinho, J.A.P. Coutinho, Tunable hydrophobic eutectic solvents based on terpenes and monocarboxylic acids, ACS Sustain. Chem. Eng. 6 (2018) 8836–8846, https://doi.org/10.1021/acssuschemeng.8b01203.

[27] C. Florindo, L. Romero, I. Rintoul, L.C. Branco, I.M. Marrucho, From phase change materials to green solvents: Hydrophobic low viscous fatty acid-based deep eutectic solvents, ACS Sustain. Chem. Eng. 6 (2018) 3888–3895, https://doi.org/10.1021/acssuschemeng.7b04235.

[28] D.J.G.P. Van Osch, L.F. Zubeir, A. Van Den Bruinhorst, M.A.A. Rocha, M.C. Kroon, Hydrophobic deep eutectic solvents as water-immiscible extractants, Green Chem. 17 (2015) 4518–4521, https://doi.org/10.1039/c5gc01451d.

[29] J.J. Li, H. Xiao, X.D. Tang, M. Zhou, Green carboxylic acid-based deep eutectic solvents as solvents for extractive desulfurization, Energy Fuel 30 (2016) 5411–5418, https://doi.org/10.1021/acs.energyfuels.6b00471.

[30] W. Pitacco, C. Samorì, L. Pezzolesi, V. Gori, A. Grillo, M. Tiecco, M. Vagnoni, P. Galletti, Extraction of astaxanthin from Haematococcus pluvialis with hydrophobic deep eutectic solvents based on oleic acid, Food Chem. 379 (2022) 132156, https://doi.org/10.1016/j.foodchem.2022.132156.

[31] W. Chen, X. Li, L. Chen, G. Zhou, Q. Lu, Y. Huang, Y. Chao, W. Zhu, Tailoring hydrophobic deep eutectic solvent for selective lithium recovery from the mother liquor of Li2CO3, Chem. Eng. J. 420 (2021) 127648, https://doi.org/10.1016/j.cej.2020.127648.

[32] H. Shaaban, A. Mostafa, A.M. Alqarni, R. Alsultan, Z. Al shehab, Z. Aljarrash, W. Al-Zawad, S. Al-Kahlah, M. Amir, Dispersive liquid-liquid microextraction utilizing menthol-based deep eutectic solvent for simultaneous determination of sulfonamides residues in powdered milk-based infant formulas, J. Food Compos. Anal. 117 (2023) 105137, https://doi.org/10.1016/j.jfca.2023.105137.

[33] ICH Harmonised Guideline, International council for harmonisation of technical requirements for pharmaceuticals for human use. Validation of analytical procedures Q2(R2), 2022.
[34] K.A. Omar, R. Sadeghi, Database of deep eutectic solvents and their physical properties: A review, J. Mol. Liq. 384 (2023) 121899, https://doi.org/10.1016/j.molliq.2023.121899.
[35] M.K. Rajput, M. Konwar, D. Sarma, Hydrophobic natural deep eutectic solvent THY-DA as sole extracting agent for arsenic (III) removal from aqueous solutions, Environ. Technol. Innov. 24 (2021) 102017, https://doi.org/10.1016/j.eti.2021.102017.
[36] A.R. Harifi-Mood, M. Sarafrazi, CO2 solubility in terpenoid-based hydrophobic deep eutectic solvents: An experimental and theoretical study, J. Environ. Chem. Eng. 11 (2023) 109177, https://doi.org/10.1016/j.jece.2022.109177.
[37] K. Zhang, R. Guo, Y. Wang, Q. Nie, G. Zhu, One-step derivatization and temperature-controlled vortex-assisted liquid-liquid microextraction based on the solidification of floating deep eutectic solvents coupled to UV–Vis spectrophotometry for the rapid determination of total iron in water and food, Food Chem. 384 (2022) 132414, https://doi.org/10.1016/j.foodchem.2022.132414.
[38] N. Schaeffer, D.O. Abranches, L.P. Silva, M.A.R. Martins, P.J. Carvalho, O. Russina, A. Triolo, L. Paccou, Y. Guinet, A. Hedoux, J.A.P. Coutinho, Non-ideality in thymol + Menthol type v deep eutectic solvents, ACS Sustain. Chem. Eng. 9 (2021) 2203–2211, https://doi.org/10.1021/acssuschemeng.0c07874.
[39] K. Li, Y. Jin, D. Jung, K. Park, H. Kim, J. Lee, In situ formation of thymol-based hydrophobic deep eutectic solvents: Application to antibiotics analysis in surface water based on liquid-liquid microextraction followed by liquid chromatography, J. Chromatogr. A 1614 (2020), https://doi.org/10.1016/j.chroma.2019.460730.
[40] A.P.R. Santana, J.A. Mora-Vargas, T.G.S. Guimarães, C.D.B. Amaral, A. Oliveira, M. H. Gonzalez, Sustainable synthesis of natural deep eutectic solvents (NADES) by different methods, J. Mol. Liq. 293 (2019) 17–20, https://doi.org/10.1016/j.molliq.2019.111452.
[41] M.F. Majid, H.F. Mohd Zaid, C.F. Kait, N.A. Ghani, K. Jumbri, Mixtures of tetrabutylammonium chloride salt with different glycol structures: Thermal stability and functional groups characterizations, J. Mol. Liq. 294 (2019) 111588, https://doi.org/10.1016/j.molliq.2019.111588.
[42] T. Khezeli, A. Daneshfar, R. Sahraei, A green ultrasonic-assisted liquid-liquid microextraction based on deep eutectic solvent for the HPLC-UV determination of ferulic, caffeic and cinnamic acid from olive, almond, sesame and cinnamon oil, Talanta 150 (2016) 577–585, https://doi.org/10.1016/j.talanta.2015.12.077.
[43] B. Ozturk, C. Parkinson, M. Gonzalez-Miquel, Extraction of polyphenolic antioxidants from orange peel waste using deep eutectic solvents, Sep. Purif. Technol. 206 (2018) 1–13, https://doi.org/10.1016/j.seppur.2018.05.052.
[44] A.P. Abbott, Application of hole theory to the viscosity of ionic and molecular liquids, ChemPhysChem 5 (2004) 1242–1246, https://doi.org/10.1002/cphc.200400190.
[45] A.P. Abbott, G. Capper, S. Gray, Design of improved deep eutectic solvents using hole theory, ChemPhysChem 7 (2006) 803–806, https://doi.org/10.1002/cphc.200500489.
[46] G. García, S. Aparicio, R. Ullah, M. Atilhan, Deep eutectic solvents: Physicochemical properties and gas separation applications, Energy Fuel 29 (2015) 2616–2644, https://doi.org/10.1021/ef5028873.
[47] B. Tang, K.H. Row, Recent developments in deep eutectic solvents in chemical sciences, Monatsh. Chem. 144 (2013) 1427–1454, https://doi.org/10.1007/s00706-013-1050-3.
[48] C. Florindo, L.C. Branco, I.M. Marrucho, Quest for green-solvent design: From hydrophilic to hydrophobic (Deep) eutectic solvents, ChemSusChem 12 (2019) 1549–1559, https://doi.org/10.1002/cssc.201900147.
[49] F. Chemat, H. Anjum, A.M. Shariff, P. Kumar, T. Murugesan, Thermal and physical properties of (Choline chloride + urea + l-arginine) deep eutectic solvents, J. Mol. Liq. 218 (2016) 301–308, https://doi.org/10.1016/j.molliq.2016.02.062.
[50] S.P. Ijardar, Deep eutectic solvents composed of tetrabutylammonium bromide and PEG: Density, speed of sound and viscosity as a function of temperature, J. Chem. Thermodyn. 140 (2020) 105897, https://doi.org/10.1016/j.jct.2019.105897.
[51] Q. Xu, L.Y. Qin, Y.N. Ji, P.K. Leung, H.N. Su, F. Qiao, W.W. Yang, A.A. Shah, H. M. Li, A deep eutectic solvent (DES) electrolyte-based vanadium-iron redox flow battery enabling higher specific capacity and improved thermal stability, Electrochim. Acta 293 (2019) 426–431, https://doi.org/10.1016/j.electacta.2018.10.063.
[52] A.P. Abbott, D. Boothby, G. Capper, D.L. Davies, R.K. Rasheed, Deep eutectic Solvents formed between choline chloride and carboxylic acids: Versatile alternatives to ionic liquids, JACS 126 (2004) 9142–9147, https://doi.org/10.1021/ja048266j.
[53] R.K. Gautam, D. Seth, Thermal conductivity of deep eutectic solvents, J. Therm. Anal. Calorim. 140 (2020) 2633–2640, https://doi.org/10.1007/s10973-019-09000-2.
[54] M. Atilhan, S. Aparicio, A review on the thermal conductivity of deep eutectic solvents, J. Therm. Anal. Calorim. 148 (2023) 8765–8776, https://doi.org/10.1007/s10973-023-12280-4.
[55] D.J.G.P. Van Osch, C.H.J.T. Dietz, S.E.E. Warrag, M.C. Kroon, The Curious case of hydrophobic deep eutectic solvents: A story on the discovery, design, and applications, ACS Sustain. Chem. Eng. 8 (2020) 10591–10612, https://doi.org/10.1021/acssuschemeng.0c00559.
[56] Prince George's Community College, Chm 2000 General Chemistry for Engineering. Chapter 9.2.: Solubility and Structure, 2023.